

# 1 Fisher Waves and the Velocity of Front Propagation in a Two-Species Invasion Model with Preemptive Competition

L. O'Malley<sup>1</sup>, B. Kozma<sup>1</sup>, G. Korniss<sup>1</sup>, Z. Rácz<sup>2</sup> and T. Caraco<sup>3</sup>

<sup>1</sup> Department of Physics, Applied Physics, and Astronomy,  
Rensselaer Polytechnic Institute, 110 8th Street, Troy, NY 12180-3590, USA  
E-mail: [omall1@rpi.edu](mailto:omall1@rpi.edu), [kozmab@rpi.edu](mailto:kozmab@rpi.edu), [korniss@rpi.edu](mailto:korniss@rpi.edu)

<sup>2</sup> Institute for Theoretical Physics - HAS,  
Eötvös University, Pázmány sétány 1/a, 1117 Budapest, Hungary  
E-mail: [racz@general.elte.hu](mailto:racz@general.elte.hu)

<sup>3</sup> Department of Biological Sciences,  
University at Albany, Albany NY 12222, USA  
E-mail: [caraco@albany.edu](mailto:caraco@albany.edu)

**Summary.** We consider an individual-based two-dimensional spatial model with nearest-neighbor preemptive competition to study front propagation between an invader and a resident species. In particular, we investigate the asymptotic front velocity and compare it with mean-field predictions.

## 1.1 Introduction and Model

The dynamics of propagating fronts are fundamental in the study of the spread of advantageous alleles, species [1], or opinions [2]. Most notably, Fisher [3] and Kolmogorov et al. [4] first addressed the velocity characteristics of a simple front by way of a reaction-diffusion equation [1], which served as a one-dimensional model for the spread of a favorable gene. Our study of front propagation envisions introduction of an advantageous allele or a competitively superior species through mutation within [5, 6] or geographic dispersal to [7, 8] a resident population, respectively. Introductions occur rarely, and stochastically in both space and time. We have shown [5–8] that the time evolution of such systems can be well described within the framework of homogeneous nucleation and growth. In particular, in two dimensions, for sufficiently large systems, the typical time scale (lifetime) until competitive exclusion of the weaker allele or species scales as  $\tau \sim (Iv^2)^{-1/3}$ , where  $I$  is the stochastic nucleation rate per unit area of the successful clusters of the better competitor and  $v$  is the asymptotic radial velocity of the corresponding circular fronts. It is, thus, clear that the full understanding of the dependence of the lifetime on the local rates of the systems requires that of the velocity of the front separating the two alleles or species. Therefore, we focus on the velocity characteristics of a two-dimensional two-species model

of invasion with preemptive competition, where the invading species has a reproductive advantage over the residents.

Here we study the velocity of the invading fronts of both planar and circular shapes on  $L_x \times L_y$  two-dimensional lattices as a function of the reproduction and mortality rates of each species, and compare them with mean-field predictions. Each lattice site can be empty or occupied by the resident or the invader. A lattice site represents the minimal amount of locally available resources which can sustain an individual. Competition for resources is preemptive, and therefore an individual site cannot be taken by either species until its occupant’s mortality makes it available. Preemptive competition is typical for plant species competing for common limiting resources [9–13]. The local occupation number at site  $\mathbf{x}$  is  $n_i(\mathbf{x}) = 0, 1, i = 1, 2$ , representing the number of resident and invader species, respectively. Due to the excluded volume constraint,  $n_1(\mathbf{x})n_2(\mathbf{x}) = 0$ , since two species cannot simultaneously occupy the same site. A species can colonize open sites through *local* clonal propagation only. An individual of either species occupying site  $\mathbf{x}$  may reproduce only if one or more of its neighboring sites is empty (here we consider nearest-neighbor interactions only).

Our unit time is one Monte Carlo step per site (MCSS) during which  $L_x L_y$  sites are chosen randomly. The occupancy (local configuration) of a chosen site is updated based on the following transition rates. When a site is empty, it can become occupied by species  $i$  of a neighboring site, at rate  $\alpha_i \eta_i(\mathbf{x})$ , where  $\alpha_i$  is the individual-level reproduction rate and  $\eta_i(\mathbf{x}) = (1/4) \sum_{\mathbf{x}' \in \text{nn}(\mathbf{x})} n_i(\mathbf{x}')$  is the density of species  $i$  around site  $\mathbf{x}$ ;  $\text{nn}(\mathbf{x})$  is the set of nearest neighbors of site  $\mathbf{x}$ . If a site is occupied by an individual, it can die at rate  $\mu$  (regardless of the species). We summarize the local transition rules for an arbitrary site  $\mathbf{x}$  as

$$0 \xrightarrow{\alpha_1 \eta_1(\mathbf{x})} 1, \quad 0 \xrightarrow{\alpha_2 \eta_2(\mathbf{x})} 2, \quad 1 \xrightarrow{\mu} 0, \quad 2 \xrightarrow{\mu} 0, \quad (1.1)$$

where 0, 1, 2 indicates whether the site is empty, or occupied by the resident, or invader species, respectively. We study the regime where  $\mu < \alpha_1 < \alpha_2$ , so that competition between the two alleles drives the dynamics and the invading species has an individual-level reproductive advantage over the resident.

For planar fronts, we consider an  $L_x \times L_y$  lattice with periodic boundary conditions along the  $y$  direction. The direction of propagation is along the  $x$  direction by virtue of the initial condition; we set a flat front separating the invader species from the residents; for simplicity, to the left (right) of the front, all sites are occupied by the invaders (residents). As the simulation begins, a number of individuals die in a few time steps, and in both domains, away from the front, the densities quickly relax to their “quasi-equilibrium” value where the clonal propagation is balanced by mortality. The competition between the two species, hence, takes place in the interfacial region. Throughout the simulation, we keep track of the location of the invading front, by defining the edge as the right-most location of an individual of species 2, for each row of our lattice. The average position of the front is then recorded for

each time step, from which one can extract the front velocity. We also studied the velocity of circular fronts on an  $L \times L$  lattice, with an initial condition of a sufficiently large central cluster of the invading species (with radius slightly larger than a critical radius [6, 8]), with all other sites occupied by the resident species. We then keep track of the time-dependent global density of the invaders, from which extracted the average radial velocity of the growing circular cluster. Before discussing our simulation results, we first consider those obtained from the mean-field equations of motion.

## 1.2 Mean-Field Equations and Propagation into an Unstable State

From the above transition rates Eq. (1.1) and the underlying master equation, neglecting correlations between the occupation numbers at different sites, for the ensemble-averaged local densities  $\rho_i(\mathbf{x}, t) \equiv \langle n_i(\mathbf{x}, t) \rangle$  one obtains

$$\begin{aligned} \rho_i(\mathbf{x}, t+1) - \rho_i(\mathbf{x}, t) &= [1 - \rho_1(\mathbf{x}, t) - \rho_2(\mathbf{x}, t)] \frac{\alpha_i}{4} \sum_{\mathbf{x}' \in \text{nn}(\mathbf{x})} \rho_i(\mathbf{x}', t) \\ &\quad - \mu \rho_i(\mathbf{x}, t), \end{aligned} \quad (1.2)$$

$i = 1, 2$ . For further insight we take a naive continuum limit of Eq. (1.2), yielding

$$\begin{aligned} \partial_t \rho_i(\mathbf{x}, t) &= \frac{\alpha_i}{4} [1 - \rho_1(\mathbf{x}, t) - \rho_2(\mathbf{x}, t)] \nabla^2 \rho_i(\mathbf{x}, t) \\ &\quad + \alpha_i [1 - \rho_1(\mathbf{x}, t) - \rho_2(\mathbf{x}, t)] \rho_i(\mathbf{x}, t) - \mu \rho_i(\mathbf{x}, t). \end{aligned} \quad (1.3)$$

Spatially homogeneous solutions of these equations,  $(\rho_1^*, \rho_2^*)$ , are  $(0, 0)$ ,  $(1 - \mu/\alpha_1, 0)$ , and  $(0, 1 - \mu/\alpha_2)$ . For  $\mu < \alpha_1 < \alpha_2$ , only the  $(0, 1 - \mu/\alpha_2)$  fixed point is stable. Thus, the motion of the invading front amounts to propagation into an unstable state [3, 4, 14–16], a phenomenon that has generated a vast amount of literature [17] since the original papers by Fisher [3] and Kolmogorov et al. [4], with applications ranging from reaction-diffusion systems [18, 19], population dynamics [1], epidemics [20] or opinion formation in social systems [2]. At the level of the mean-field equations, the front is “pulled” by its leading edge, and for sufficiently sharp initial profiles, the asymptotic velocity  $v$  is determined by this infinitesimally small density of invaders intruding into the linearly unstable, resident-dominated regime. Performing standard analysis on Eqs. (1.3), one obtains the velocity of the “marginally” stable invading fronts [1, 15–17]

$$v^* = \frac{\mu}{\alpha_1} \sqrt{\alpha_2(\alpha_2 - \alpha_1)}. \quad (1.4)$$

Thus, for small differences in the local reproduction rates,  $v^* \sim (\alpha_2 - \alpha_1)^\theta$  with  $\theta = 1/2$ . Equation (1.4) reproduces the velocity obtained by numeri-

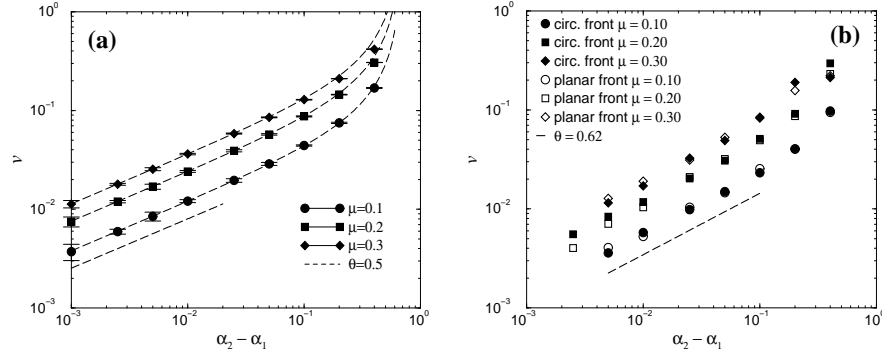


**Fig. 1.1.** (a) Front velocity obtained by numerical iteration of the mean-field equations (1.2), for fixed  $\alpha_2=0.70$ , as a function of the difference of propagation rates,  $\alpha_2-\alpha_1$ , for three different values of  $\mu$ . The dashed curves are the analytic velocities of the “marginally stable” fronts, given by Eq. (1.4); the dashed straight line segment corresponds to the slope  $\theta=0.5$ . (b) Front velocity from Monte Carlo simulations for fixed  $\alpha_2=0.70$  as in (a), with  $L_x=1000$ ,  $L_y=100$ , for planar, and  $L_x=L_y=1000$  for circular fronts, for three values of  $\mu$ . The dashed straight line segment corresponds to the effective power law with an exponent  $\theta\approx 0.62$  for small differences between the local reproduction rates.

cally iterating the discrete-time discrete-space continuous-density mean-field equations (1.2) remarkable well, as shown in Fig. 1.1(a).

### 1.3 Monte Carlo Results and Discussion

We performed dynamic Monte Carlo simulations using the local rates given by Eq. (1.1). In the case of planar fronts, we found that the front velocity is much smaller than that of the mean-field approximation [Fig. 1.1(b)]. Further, for small differences between the local reproduction rates,  $v^* \sim (\alpha_2 - \alpha_1)^\theta$  with  $\theta \approx 0.62$ , an exponent significantly differing from the mean-field scaling [Fig. 1.1]. Results from the simulations of the propagation of circular fronts closely match those of the planar fronts. A recent study [20] has found a similar behavior in a discrete two-dimensional stochastic epidemic model.

The discreteness of the individuals (or equivalently, effective density cut-offs in a continuum description) [21–23] and noise [24, 25] have been shown to produce velocity characteristic drastically different from those of the mean-field equations. More precisely, advancing fronts in stochastic individual-based or particle models, which in the mean-field limit converge to a pulled front behavior, are instead “pushed” [17]. That is, the front velocity is determined by the full non-linearity of the frontal region, as opposed to the infinitesimally small leading edge [17]. Our model provides an example for this generic behavior.

## Acknowledgments

G.K. is grateful for discussions with Eli Ben-Naim and for the hospitality of CNLS at the Los Alamos National Laboratory, where some of this work was initiated. This research was supported in part by the US NSF through Grant Nos. DEB-0342689 and DMR-0426488. Z.R. has been supported in part by the Hungarian Academy of Sciences through Grant OTKA-T043734.

## References

1. J.D. Murray: *Mathematical Biology I and II, 3rd edition* (Springer-Verlag, New York, 2002, 2003)
2. E. Ben-Naim: *Europhys. Lett.* **69**, 671 (2005)
3. R.A. Fisher: *Annals of Eugenics* **7**, 355 (1937)
4. A.N. Kolmogorov, I. Petrovsky, N. Piskounov: *Moscow Univ. Bull. Math.* **1**, 1 (1937)
5. J.A. Yasi, G. Korniss, T. Caraco: in *Computer Simulation Studies in Condensed Matter Physics XVIII*, edited by D.P. Landau, S.P. Lewis, and H.-B. Schüttler, Springer Proceedings in Physics (Springer-Verlag, Berlin, 2006, in press).
6. L. O'Malley, J. Basham, J.A. Yasi, G. Korniss, A. Allstadt, T. Caraco: submitted to *Theor. Popul. Biol.* (preprint, 2005); arXiv:q-bio/0602023
7. G. Korniss, T. Caraco: *J. Theor. Biol.* **233**, 137 (2005)
8. L. O'Malley, A. Allstadt, G. Korniss, T. Caraco: in *Fluctuations and Noise in Biological, Biophysical, and Biomedical Systems III*, edited by N.G. Stocks, D. Abbott, and R.P. Morse, Proceedings of SPIE Vol. 5841 (SPIE, Bellingham, WA, 2005) pp. 117–124.
9. J.B. Shurin, P. Amarasekare, J.M. Chase, R.D. Holt, M.F. Hoopes, M.A. Leibold: *J. Theor. Biol.* **227**, 359 (2004)
10. P. Amarasekare: *Ecol. Lett.* **6**, 1109 (2003)
11. D.W. Yu, H.B. Wilson: *Am. Nat.* **158**, 49 (2001)
12. D.E. Taneyhill: *Ecol. Monogr.* **70**, 495 (2000)
13. B. Oborny, G. Meszéna, G. Szabó: *Oikos* **109**, 291 (2005)
14. D.G. Aronson, H. F. Weinberger: *Adv. Math.* **30**, 33 (1978)
15. G. Dee, J. S. Langer: *Phys. Rev. Lett.* **50**, 383 (1983)
16. W. van Saarloos, *Phys. Rev. Lett.* **58**, 2571 (1987)
17. W. van Saarloos: *Phys. Rep.* **386**, 29 (2003)
18. J. Riordan, C.R. Doering, D. ben-Avraham: *Phys. Rev. Lett.* **75**, 565 (1995)
19. D. ben-Avraham: *Phys. Lett.* **247**, 53 (1998)
20. C.P. Warren, G. Mikus, E. Somfai, L.M. Sander: *Phys. Rev. E* **63**, 056103 (2001)
21. E. Brunet, B. Derrida: *Phys. Rev. E* **56**, 2597 (1997)
22. D.A. Kessler, Z. Ner, L.M. Sander: *Phys. Rev. E* **58**, 107 (1998)
23. D.A. Kessler, H. Levine: *Nature* **394**, 556 (1998)
24. C.R. Doering, C. Mueller, P. Smereka: *Physica A* **325**, 243 (2003)
25. J.G. Conlon, C.R. Doering: *J. Stat. Phys.* **120**, 421 (2005)